AIP Advances

Phononic crystals and elastodynamics: Some relevant points

N. Aravantinos-Zafiris, M. M. Sigalas, M. Kafesaki, and E. N. Economou

Citation: AIP Advances **4**, 124203 (2014); doi: 10.1063/1.4904406
View online: http://dx.doi.org/10.1063/1.4904406
View Table of Contents: http://scitation.aip.org/content/aip/journal/adva/4/12?ver=pdfcov
Published by the AIP Publishing

Phononic crystals and elastodynamics: Some relevant points

N. Aravantinos-Zafiris,[1,2] M. M. Sigalas,[1] M. Kafesaki,[3,4] and E. N. Economou[3,5]
[1]*Dept. of Materials Science, University of Patras, Patras 26504, Greece*
[2]*Department of Sound and Musical Instruments Technology, Ionian Islands Technological Educational Institute, Lixouri, 28200, Greece*
[3]*Institute of Electronic Structure and Laser (IESL), Foundation for Research and Technology, Hellas (FORTH), P.O. Box 1387, 70013 Heraklion, Crete, Greece*
[4]*Dept. of Materials Science and Technology, Univ. of Crete, Greece*
[5]*Dept. of Physics, Univ. of Crete, Greece*

(Received 18 September 2014; accepted 24 November 2014; published online 12 December 2014)

In the present paper we review briefly some of the first works on wave propagation in phononic crystals emphasizing the conditions for the creation of acoustic band-gaps and the role of resonances to the band-gap creation. We show that useful conclusions in the analysis of phononic band gap structures can be drawn by considering the mathematical similarities of the basic classical wave equation (Helmholtz equation) with Schrödinger equation and by employing basic solid state physics concepts and conclusions regarding electronic waves. In the second part of the paper we demonstrate the potential of phononic systems to be used as elastic metamaterials. This is done by demonstrating negative refraction in phononic crystals and subwavelength waveguiding in a linear chain of elastic inclusions, and by proposing a novel structure with close to pentamode behavior. Finally the potential of phononic structures to be used in liquid sensor applications is discussed and demonstrated. [http://dx.doi.org/10.1063/1.4904406]

I. INTRODUCTION: WAVES IN PERIODIC MEDIA – A SHORT CHRONOLOGY

The first quantitative study of wave propagation in a periodic medium was considered and published by Newton[1] in 1686. The model system was a one-dimensional chain of identical masses connected with identical springs between nearest-neighbors. This discrete system was used for deducing the sound velocity in air. Subsequently, Newton's model and its extensions were studied in the 18th, 19th, and 20th centuries by several researchers. This early literature is briefly presented in the excellent book by Brillouin[2] where the mathematical equivalence of the wavy propagation of displacements in mechanical periodic systems (both discrete and continuous), of electrical current in periodic electrical lines, and of the electronic wavefunction in crystals was recognized and exploited. A milestone in this long process towards understanding wave propagation in periodic media was the Floquet theorem for one-dimensional systems and its extension by Bloch in 1928, who applied it to the motion of electrons in crystalline solids marking the birth of modern Solid State Physics[3,4] based on the concepts of bands and gaps (pass and stop bands in engineering terminology). The knowledge of electronic motion in solids was supplemented by the understanding of the ionic motion obtained by a three-dimensional extension of the old Newton model. The development of Solid State Physics was followed by the discovery of transistor in 1948 and the subsequent technological explosion. From the conceptual point of view, the next milestone was the study of the consequences on the electronic motion of gradually introducing disorder in a periodic crystal. Anderson in a seminal paper of 1958[5] proposed that disorder, if strong enough, may localize the electrons, i.e. may trap them in a finite region of space leading thus to a disorder induced metal-insulator (M-I) transition. Temperature and correlation effects play

also a complicated role in the process of M-I transition. This difficulty led some researchers to exploit the underlying mathematical similarity between electronic waves and classical waves such as electromagnetic, acoustic, and elastic waves for wavelengths much larger than atomic scale, where each individual material exhibits a simple behavior free of the correlation and temperature effects which make the study of disorder induced localization for electrons very complicated. However, it was soon realized that electromagnetic (EM) waves interact rather weakly with matter (apart from absorption) as to create conditions of effectively strong disorder; as a remedy to this difficulty, it was proposed to create first a periodic system in which the EM wave propagation will exhibit bands and gaps. Then, the idea was, that by disordering this periodic system the gaps will be filled by states, which can be easily localized. Thus, following this path, some researchers ended up with the problem of designing and fabricating a composite system (of at least two components) which will exhibit gaps (and hence bands) for the propagation of EM waves. After several attempts[6] the problem was solved even in the optical regime and for thee-dimensions.[7–9] It was soon realized that a composite system exhibiting gaps and bands for EM waves was much more important from the point of view of both basic physics and applications than the original problem. Thus the very active and still fast growing field of Photonic Crystals was created.

Sigalas and Economou in 1992 proposed that gaps and bands in properly designed composite systems can appear in the propagation of acoustic and elastic waves.[10] They considered a three-dimensional periodic structure of identical non-touching spheres arranged in fcc, bcc, sc, diamond, and hex lattices and calculated the full band structure for both acoustic (where both the host and the spheres are fluids) and elastic (where both the host and the spheres are solids) waves. Elastic waves from one point of view appeared more favorable than EM waves for gap creation because each component possesses three material parameters (density, ρ, longitudinal, c_l, and transverse, c_t, velocities) vs two for EM (permittivity and permeability), while on the other hand for a full gap to appear in elastic waves the gaps for transverse and longitudinal components must overlap. This initial paper[10] was followed by several others in the 90s and the field of Phononic Crystals and later the related field of Phononic Metamaterials grew tremendously, driven also by many applications.

In our quest for composite systems exhibiting phononic gaps several parameters other than the three material ones (for each component) play a role: One such parameter is the topology which usually is either of the cermet type or the network type. In the cermet topology the phononic system consists of a host material in which identical inclusions are embedded and usually arranged in a periodic way. The inclusions can be of any shape or composition but do not touch each other so that each inclusion is completely surrounded by the host material. The latter forms a continuous network so that any two points in the host can be joined by lines lying entirely within the host. In the network topology the "inclusions" are connected to each other so that any two points also in inclusions can be joined by lines laying entirely within the inclusions; in the network topology the distinction between host and inclusions may not be meaningful anymore. However, the term "inclusions" is still used for the component which occupies the smaller volume fraction. An example of cermet topology is the case of bubbles in water.[11] An example of network topology is the so-called layer-by-layer structure (known also as woodpile structure) proposed by the Iowa group[8,12] and shown in Fig. 1.

Other parameters which influence the appearance and the size of gaps are the lattice structure formed by the inclusions, the geometrical shape of the latter and their volume fraction. Usually the host material is air, or a liquid, or a solid material. The inclusions in most of the cases consist also of a single material (air, liquid, or solid) but in some cases are of composite nature, e. g. coated spheres.

In the present paper we review some important issues and some older and recent results concerning the wave propagation in phononic crystals and we comment on the conditions for the creation of phononic band gaps. Moreover, we present some recent results on phononic systems, demonstrating interesting metamaterial properties and capabilities in such systems, such as negative refraction, subwavelegth guiding, and sensing.

More specifically, the rest of the paper is organized as follows: In Section II we discuss the role of single particle resonances in the propagation characteristics of a periodic phononic, and in general classical, system; in Section III we present a short review of the methods for the solution of acoustic and elastic wave equations in isotropic media, which are shared also by the EM wave equation, and

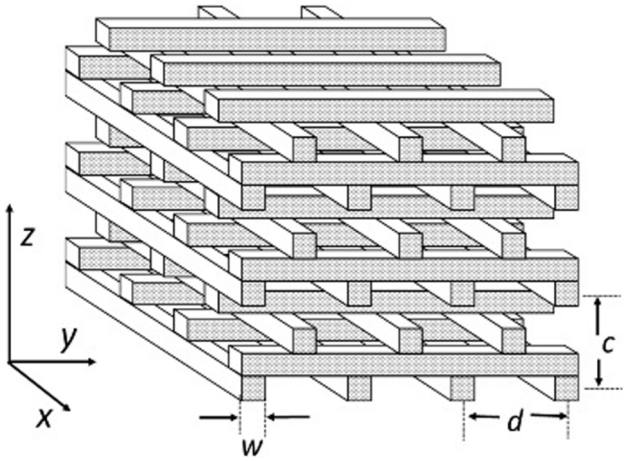

FIG. 1. The layer-by-layer structure.[8,12]

in Section IV we present some important results and conclusions regarding band and gap formation in phononic crystals. To analyze some of those results we evoke similarities of the classical wave equation (to which the solution of acoustic and elastic wave equations is reduced) with Schrödinger equation. The second part of the paper (Section V) concerns phononic systems as metamaterials. There we demonstrate negative refraction and pentamode-like behavior in different phononic crystals, subwavelength propagation in a chain of elastic scatterers showing strong sub-wavelength resonances, and the potential of phononic crystals to act as efficient liquid sensors. The paper ends with our conclusions and perspectives of the phononic crystal research.

II. THE ROLE OF RESONANCES

We consider here a two-component phononic system of the cermet topology. Since band gap creation is a result of strong scattering and destructive interference of the multiply scattered waves, a necessary (but not sufficient) condition for such a system to exhibit gaps in the propagation of acoustic or elastic waves is the following: The scattering cross-section σ_{sc} of such a wave by a single inclusion embedded in the host material must be sufficiently large, meaning that it must be considerably larger than the inclusion's geometric cross-section, s_g. For this to occur the material parameters of the inclusion must be quite different from those of the host. Even if this condition is satisfied the ratio σ_{sc} / s_g is not everywhere (i.e. for all frequencies) larger than one. Quite often it exhibits peaks at certain frequencies and in between these peaks the values of the ratio σ_{sc} / s_g frequently can be less than one. If these peaks are pronounced enough we call them resonances. A resonance is characterized by its maximum value and by its width at half maximum. The larger the ratio maximum/width, the more pronounced the resonance is. A pronounced resonance resembles a bound state in the sense that the incoming wave is trapped around the scatterer for a long time (but not infinite, as in the bound state case) and, spatially, is concentrated around the scattering center (but does not decay exponentially for large distances as in the bound state case). Periodic arrangement of strong scatterers may facilitate the creation of gaps, since it may lead to systematic destructive interference. Resonances are of two types: One is of geometric nature (Mie resonance), which depend strongly on the ratio λ_{in} / d, where λ_{in} is the wavelength within the inclusion and d is the linear size of the inclusion; in simple cases this type of resonance occurs when $\lambda_{in} / 2d \approx 1 / n$, where n is positive integer. However, in the case of elastic waves the situation is considerably more complicated, since the scattering cross-sections for longitudinal or transverse incoming waves are given by different and rather complicated expressions even for homogeneous inclusion of simple geometrical shape such as spherical.[13] The second type of resonances is usually independent or weakly dependent on the wavelength, but strongly dependent on the frequency as a result of the inclusions possessing eigenfrequency(ies) associated with their

very nature or structure. An example of this type is the case of a lead spheres coated with a rubber and embedded in an epoxy host.[14]

III. WAVE EQUATIONS AND METHODS FOR THEIR SOLUTIONS

To reach conclusions for the elastic and acoustic wave equation in isotropic composites and their solutions we often, following Brillouin's approach, exploit their mathematical similarities with Schrödinger equation and/or electromagnetic wave equation. Hence, in order to easily explore and refer to such similarities, we present all the basic, wave-related partial differential equations of physics.

Schrödinger scalar equation:

$$\nabla^2\psi(\mathbf{r}) + (2m/\hbar^2)[E - \mathcal{V}(\mathbf{r})]\,\psi(\mathbf{r}) = 0. \tag{3.1}$$

In Eq. (3.1) ψ is the wavefunction, m is the mass of the particle, $\hbar = h/2\pi$ is the reduced Planck's constant, $\mathcal{V}(\mathbf{r})$ is the potential energy experienced by the particle, and E is its total energy.

Helmholtz scalar equation:

$$\nabla^2 u(\mathbf{r}) + [\omega^2 / c(\mathbf{r})^2]\,u(\mathbf{r}) = 0. \tag{3.2}$$

ω is the angular frequency and $c(\mathbf{r})$ is the velocity of the wave.

Acoustic waves in isotropic fluids:

$$\nabla[\lambda(\mathbf{r})\nabla\cdot\mathbf{u}(\mathbf{r})] + \rho(\mathbf{r})\,\omega^2\mathbf{u}(\mathbf{r}) = 0, \qquad \nabla\times\mathbf{u}(\mathbf{r}) = 0, \tag{3.3a}$$

Here $\mathbf{u}(\mathbf{r})$ is the displacement vector, $\rho(\mathbf{r})$ is the density, and $\lambda(\mathbf{r})$ is one of the Lamé coefficients.[15] By introducing the pressure, $p(\mathbf{r}) \equiv -\lambda(\mathbf{r})\nabla\cdot\mathbf{u}(\mathbf{r})$, the above equation becomes

$$\nabla[\frac{1}{\rho(\mathbf{r})}\nabla p(\mathbf{r})] + \frac{\omega^2}{\lambda(\mathbf{r})}p(\mathbf{r}) = 0. \tag{3.3b}$$

Elastic waves in isotropic solids (summation over repeated indices is implied):

$$\mu\nabla^2\boldsymbol{u} + \mu\nabla(\nabla\cdot\mathbf{u}) + \lambda\nabla(\nabla\cdot\mathbf{u}) + (\nabla\lambda)(\nabla\cdot\mathbf{u}) + \frac{\partial\mu}{\partial x_k}(\frac{\partial\mathbf{u}}{\partial x_k}) + \frac{\partial\mu}{\partial x_k}(\nabla u_k) = -\omega^2\rho\,\mathbf{u} \tag{3.4}$$

In Eq. (3.4) μ is the other Lamé coefficient.[15] Lamé coefficients are connected with the longitudinal and transverse sound velocities in homogeneous media as follows:[15] $c_l = \sqrt{(\lambda + 2\mu)/\rho}$, $c_t = \sqrt{\mu/\rho}$.

Electromagnetic waves:

$$\nabla\times[\varepsilon(\mathbf{r})^{-1}\nabla\times\mathbf{H}(\mathbf{r})] = \omega^2\mu(\mathbf{r})\,\mathbf{H}(\mathbf{r}), \quad \nabla\cdot[\mu(\mathbf{r})\mathbf{H}(\mathbf{r})] = 0. \tag{3.5}$$

Here $\mathbf{H}(\mathbf{r})$ is the auxiliary magnetic field, $\varepsilon(\mathbf{r})$ is the permittivity, and $\mu(\mathbf{r})$ is the permeability.

Notice that, if the density $\rho(\mathbf{r})$ is a constant, Eq. (3.3b) is reduced to Eq. (3.2) and, therefore, becomes mathematically equivalent to Schrödinger equation. In the next section we shall exploit this equivalence and results from Solid State Physics to reach conclusions regarding the appearance of gaps in the Helmholtz equation (3.2).

There are several methods for solving the above equations in inhomogeneous media. All of them involve at some stage numerical techniques and some approximations which usually are controlled. For periodic systems, the most common method is the Plane Wave Expansion (PWE), according to which the known coefficients in Eqs. (3.2) to (3.5) are expanded in Fourier series and for the unknown yet fields the Bloch theorem is applied. Another method is based on the calculation of the scattering amplitude by a single inclusion for an incident wave which, however, involves the scattered waves from all other inclusions. If the system is periodic, by using the Bloch theorem, the resulting set of equations can be solved by an approach well known in Solid State Physics under the initials KKR; if there is no periodicity, only systems of not so large size can be solved by this method known as Multiple Scattering Formalism (MSF). A successful application of the multiple scattering formalism

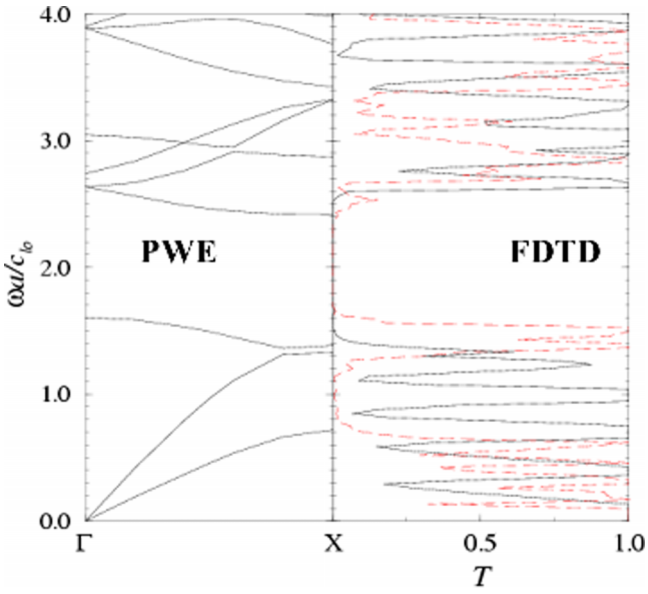

FIG. 2. Comparison of the results of the PWE and the FDTD methods for a system of Pb cylinders arranged in a square lattice within epoxy host. The volume fraction of the cylinders is 28%, a is the lattice constant and c_{lo} the longitudinal wave velocity in epoxy. The PWE result shows the band-diagram for the ΓX direction, while the FDTD result shows the transmission coefficient (T) as a function of frequency for longitudinal (solid-line) and for transverse (dashed-line) incident waves impinging upon a finite along propagation direction system of 10 unit cells. Both results demonstrate a large gap the size of which over mid-gap frequency, $\Delta\omega/\omega$, is 40%. The material parameters used in the calculation are: for Pb: ρ=11357 kgr/m^3, c_l=2158 m/s, c_t = 860 m/s; for epoxy: ρ=1180 kgr/m^3, c_l=2540 m/s, c_t = 1160 m/s.

was applied[16] to a system of glass spheres placed randomly in a water host and studied experimentally by J. H. Page *et al*.[17] We mention also the Transfer Matrix (TM) formalism which is a combination of the multiple scattering method applied to two-dimensional planes and the transfer matrix approach from plane to the next plane.[18] Finally, an extensively used method is the Finite Difference Time Domain (FDTD) which solves numerically the time dependent equation resulting from equations (3.2) to (3.5) by replacing ω^2 by $-\partial^2/\partial t^2$ and taking the Fourier transform of the time dependent solutions. It is worth-mentioning here that the FDTD method shows great power not only in the calculation of the eigensolutions of the wave equation for infinite periodic systems but mainly in calculating the response of finite systems, both periodic and random, to an incoming incident wave. (MSF and TM methods show also the same potential.) In Fig. 2 we show and compare representative results of the PWE method and the FDTD.

IV. PHONONIC CRYSTALS AND PHONONIC BAND GAPS

A. Equivalence of classical/acoustic wave equation and Schrödinger equation

As was mentioned earlier, to conclude about the existence of bands and gaps in a periodic elastic or acoustic system we often exploit similarities between Helmholtz equation (in which the solution of elastic and acoustic wave equations can be recast under certain conditions) with Schrödinger equation.

By inspection of these two equations, Schrödinger (3.1) and Helmholtz (3.2), it is clear that there is the following correspondence: $(2m/\hbar^2)[E - \mathcal{V}(\mathbf{r})] \Leftrightarrow [\omega^2/c(\mathbf{r})^2]$. It follows from the positiveness of $\omega^2/c(\mathbf{r})^2$ that for gaps to appear in Eq. (3.2), gaps must exist in Eq. (3.1) for E larger than the maximum value $\mathcal{V}_M$ of the potential energy $\mathcal{V}(\mathbf{r})$; usually we chose the zero of energy to coincide with $\mathcal{V}_M : \mathcal{V}_M = 0$. Moreover, a local increase of $\mathcal{V}_M - \mathcal{V}(\mathbf{r})$, such as the creation of a potential well, corresponds to a local decrease of$c(\mathbf{r})^2$, i.e. to a local introduction of an inclusion of lower sound velocity than the host. Since a potential well tends to pull out of the conduction band and into the gap a local eigenstate,[19] it is implied that (in the presence of an already existing gap) an extra local

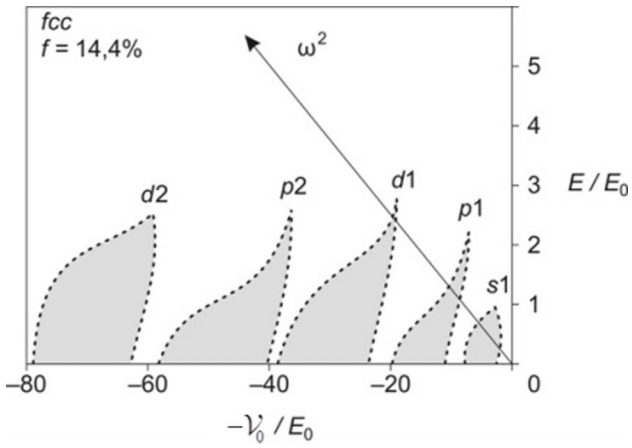

FIG. 3. The shaded regions in the plane, energy vs depth of the potential, correspond to electronic gaps for $E>0$. Each such region is dominated by the indicated spherical harmonic. The ω^2 axis for the Helmholtz equation is also shown; its slope is equal to $[1-(c_h/c_i)^2]^{-1}$, with $c_h > c_i$ $E_0 = \hbar^2/2m\,a^2$.

region of smaller sound velocity tends to pull out of the upper band an eigenmode localized around this lower velocity region and of frequency in the upper part of the gap. In contrast (in the presence of an already existing gap), an extra local region of higher speed of sound tends to push up and out of the lower band an eigenmode localized around this extra region and of frequency in the lower part of the gap. Examples of such a behavior are presented in Ref. 9.

In Fig. 3 it is shown how the results of the electronic case (characterized by a, $(E\,/\,E_0)$, $-(\mathcal{V}_0/E_0)$, the volume fraction f, and the lattice structure, where $E_0 \equiv \hbar^2/2m\,a^2$) can be used for reaching conclusions regarding the Helmholtz equation (characterized by a, ω^2, c_h, c_i the volume fraction f, and the lattice structure).[20,4] The shaded regions are the regions of gaps for positive energies E (i.e. $E>\mathcal{V}_M = 0$) for a periodic electronic system where $\mathcal{V}(\mathbf{r}) = -\mathcal{V}_0\,(\mathcal{V}_0 > 0)$ for $\mathbf{r}$ inside any of the identical spherical regions of radius a arranged in a fcc lattice and $\mathcal{V}(\mathbf{r}) = 0$ for $\mathbf{r}$ outside these spherical regions. The correspondence between the Schrödinger and the Helmholtz equations are: $E/E_0 \Leftrightarrow \omega^2 a^2/c_h^2$, $-\mathcal{V}_0/E_0 = \omega^2 a^2[1-(c_h/c_i)^2]/c_h^2$, with $E_0 = \hbar^2/2m\,a^2$. Thus the highest the contrast between the velocities of sound in the host, c_h, and the inclusions, c_i, the closer the ω^2 axis in Fig. 3 comes to the horizontal axis and, therefore, more and wider gaps appear in the Helmholtz case.

B. Relation between gaps of a periodic system and scattering cross-section by a single inclusion

It has been shown[21] that large gaps appear in elastic wave propagation in periodic composites composed of solid host/solid inclusions when the mass density of the inclusions is much higher than that of the host and their sound velocities are comparable to or even larger than those of the host. In this case quite often the scattering cross-section by a single inclusion as a function of frequency shows a behavior as in Fig. 4, where the peaks are due to resonances (usually Mie type).[13]

To reveal the hidden meaning of this frequency dependence of the single inclusion scattering cross-section we repeat the cross-section calculations in a system where the inclusion has been replaced by a rigid material (with $\rho \to \infty$, $\lambda \to \infty$, $\mu \to \infty$, $c_l \to 0$, $c_t \to 0$, where λ and μ are the Lame coefficients) of the same shape and size. This second calculation is very useful because it helps to identify in each frequency region whether the propagation in the periodic system takes place by employing mainly the host material or the inclusions.

The above mentioned analysis showed that the rather high cross-section values (background scattering) between the peaks of the cross-section shown in Fig. 4 are attributed to propagation of the wave by avoiding the inclusion. A representative realistic case where this picture applies is the case shown in Fig. 5, concerning an Ag spherical inclusion in epoxy host,[22,23] where $\rho_i/\rho_h = 9.83$. The cross-section by such an inclusion is shown in Fig. 5(a), while in Fig. 5(b) the scattering cross-section is recalculated

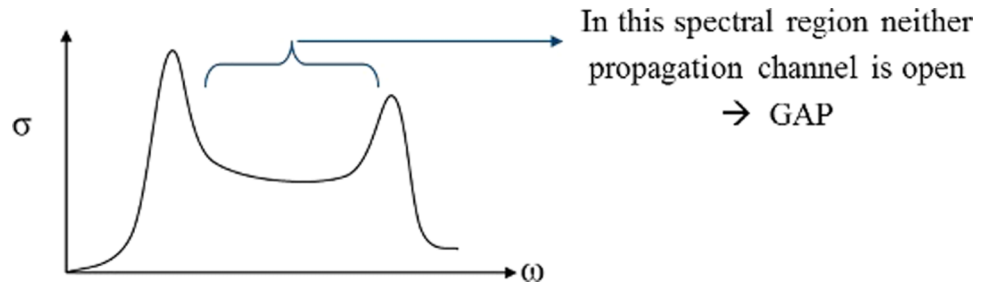

FIG. 4. Schematic plot of a typical behavior of the scattering cross-section by a single inclusion vs frequency for the case where the inclusion mass density is much higher than that of the host and their sound velocities are of the same order of magnitude.

with the inclusion replaced by rigid material ($\rho \to \infty,\ \lambda \to \infty,\ \mu \to \infty,\ c_l \to 0,\ c_t \to 0$), which, as such, does not allow the penetration of the field in its interior.

In the rigid case the peaks disappear (see Fig. 5(b)) and the scattering cross-section is almost independent of the frequency and about equal to the value between the peaks in Fig. 5(a). In Fig. 5(c) the cross-section obtained as the square of the absolute value of the difference between the scattering amplitudes of Figs a and b is plotted; it confirms that the high cross-section values between the resonances are due to propagation exclusively through the host material. This single scattering behavior leads us to the following picture for the elastic wave propagation in a system where the much heavier than the host inclusions have been arranged in a periodic lattice: There are two channels of propagation. The first one is utilizing almost entirely the host material and avoids the inclusions; it is the dominant one for frequencies between the peaks in the single scattering cross-section. The second channel is utilizing the resonances of the inclusions and propagates by hopping from one resonance to the identical ones of the neighboring inclusions in a way similar to the propagation of electrons in solids through a Linear Combination of Atomic Orbitals (LCAO); this second channel is dominant for frequencies around the resonances. If both of these channels are not contributing (the second one does not exist far away from the resonances and the first one is almost blocked if the scattering cross-section between resonances is very high), then a gap is expected. The conclusion is that for gaps to appear in periodic systems, the single scattering cross-section must exhibit resonances further away from each other with a high background scattering cross-section between them. The gap is expected to occur for

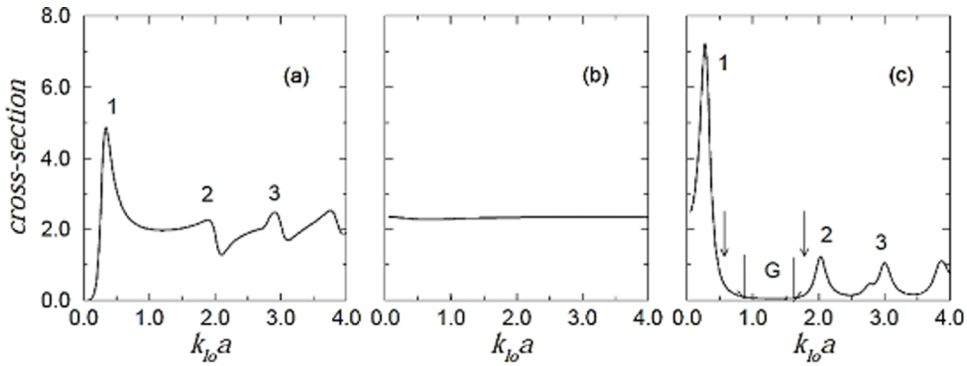

FIG. 5. (a) The scattering cross-section over the geometrical cross-section vs frequency for a spherical inclusion of silver of radius a in epoxy, where the subscript $_o$ denotes the host material (out) and a is the inclusion radius. (b) The same as in panel (a) for the silver sphere replaced by a rigid sphere. (c) The scattering cross-section corresponding to the difference between the scattering amplitude of (a) and the scattering amplitude of (b) (for details of this calculation see Ref. 13); it is shown that the background between resonances 1 and 2 is almost entirely due to propagation avoiding the inclusion. The region G in (c) between the two half-arrows is a gap region for a composite made of silver inclusions arranged in an fcc lattice of f=0.35 in epoxy host. The Ag material parameters used in the calculation are ρ=10416 kgr/m^3, c_l=3650 m/s, c_t=1610 m/s. The figure is reprinted with permission from Ref. 22.

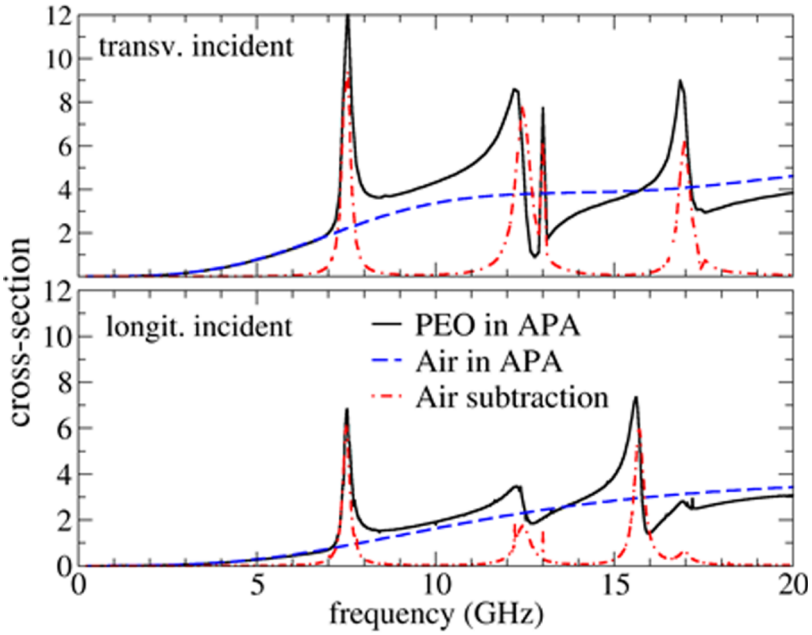

FIG. 6. Solid lines represent scattering cross-section by a single solid cylinder of PEO embedded in APA host (see text) for transverse (upper panel) and longitudinal (lower panel) incident wave. Dashed lines are for the case where the PEO has been replaced by air. Dashed-dotted line is the scattering cross-section obtained by employing as scattering amplitude the difference of the scattering amplitudes of the previous two cases. The wave velocities employed in the calculation are for APA c_l=7300 m/s, c_t=4300 m/s and for PEO c_l=1300 m/s and $c_t \to 0$. The cylinder radius is a=50 nm. The cross-section is in dimensionless units of πa^2.

frequencies corresponding to this region between resonances. It follows that for the gap to be wide the resonances must not be close to each other. Large ratios of sound velocities contrast between host and inclusions, c_{lh} / c_{li}, tends to bring the resonances closer together and, therefore, to shrink the gap or eliminate it. To emphasize, we repeat that this picture is confirmed by the results shown in Fig. 5 of Ref. 23, especially Fig. 5(c) where the wide frequency region between the resonances almost coincides with the gap region denoted by G.

In Fig. 6 the same analysis as in Fig. 5 is applied for a case of a two-dimensional fluid/solid system composed of poly-ethylene oxide (PEO) cylinders in anodic porous alumina (APA) host,[24] where, in contrast to the previous case of Ag in epoxy, the density of the inclusions (ρ = 1045 kg m^{-3}) is much smaller than that (ρ = 3700 kg m^{-3}) of the host. In the present case to analyze the propagation paths one may attempt to replace the inclusion (not by a rigid sphere) but by air sphere representing the limiting case where the density of the inclusions tends to zero. By inspection of Fig. 6 and on the basis of the previous analysis we would expect a rather wide gap in the region around 10 GHz, since there the scattering cross-section for air is at least twice as large as the geometric cross-section and the resonances are not located nearby (their frequencies are around 7.5 GHz for the lower one and around 12.5 GHz for the upper one).

However, both experimental data and numerical simulations in two-dimensional hexagonal periodic system of PEO cylinders in APA[24] have shown no gap at all, although a very pronounced flat dispersion relation was exhibited at 7.5 GHz and a less pronounced one at 12.5 GHz. Such a pronounced flatness in the dispersion relations indicates the presence of a strong resonance in agreement with the results of Fig. 6. On the other hand, the absence of gap around 10 GHz requires an explanation. We think that the different behavior in gap formation between the cases of Figs 5 and 6 is due to the essential difference between a rigid inclusion (which allows no displacement either in its interior or at its interface with the host) and an empty space (which allows no field in its interior, but easily permits displacements of the host at its interfaces). As a result of this difference the propagation in the case of vacuum inclusions does not imply exclusive utilization of the bulk or the host but involves

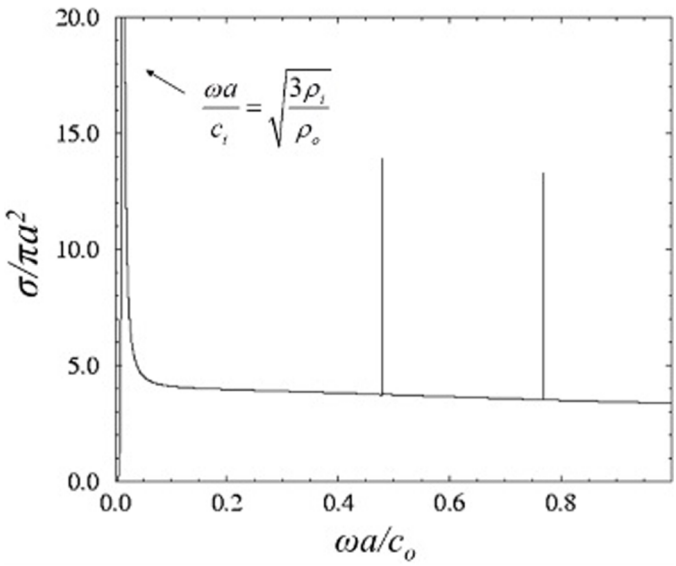

FIG. 7. Dimensionless scattering cross-section by a spherical air bubble of radius a in water as a function of the dimensionless frequency $\omega\, a/c_0$, where c_0 is the sound velocity in water. Notice the very strong resonance at low frequency (Minnaert resonance) due to the uniform compression of the bubble.

the contribution of the interfaces. Consequently the argument of only two channels of propagation breaks down.

The role of vacuum or air inclusions becomes even more pronounced in the case where the host is liquid, as in the particular example of bubbly water.[11] In Fig. 7 the scattering cross-section by a single bubble in water is shown.[4] A very strong resonance at low frequency, called Minnaert resonance, appears.

The frequency of this resonance, $f = (3174/a)$ Hz, with a in mm, is determined by the sound velocity in air (c_i) and by the ratio of densities between the two materials. This resonance is so strong that dominates the sound propagation in bubbly water even if the volume fraction occupied by the bubbles is very low. Other extremely sharp resonances are also present as shown in Fig. 7.

In Fig. 8(a) we show the band structure of periodic arrangement of air bubbles in water for air volume fraction of only 1%.[11] Notice the lowest band exhibiting a sound velocity of only 90 m s^{-1}. This very low value can be understood in terms of the relation $c = \sqrt{B_{eff} / \rho_{eff}}$, where the effective bulk modulus, B_{eff} (equal to the Lame coefficient λ_{eff} for fluids), is controlled to a large extent by the compressibility of air, while the effective density, ρ_{eff}, is essentially that of water. There is also a wide gap starting just above the Minnaert frequency and terminating at about $\omega\, a/c_0 \approx 2$. The existence of a gap is confirmed by the calculation of the transmission coefficient through a slab of bubbly water containing $7 \times 7 \times 3$ bubbles, which is shown in Fig 8(b) for both periodic and random systems. Because of the very strong scattering the multiple scattering effects play crucial role in the wave propagation through this system even for very low frequencies and low bubble volume fractions. To illustrate this point we did the same calculation in Fig. 8(c) as in Fig. 8(b) but without multi scattering effects, i.e. by assuming that the incoming wave is scattered only once. The low frequency results in Fig. 8(c) are in complete disagreement with the actual ones proving thus the crucial role of multiple scattering even for this very low volume fraction of bubbles.

C. The role of topology and lattice structure in gap formation

In periodic systems and for a particular direction of the crystal wavevector **k** there are always gaps. The concept of gap the way we are using it in the present work means that it is present for all directions of **k**. If there were spherical symmetry in the lattice, a gap in a particular direction

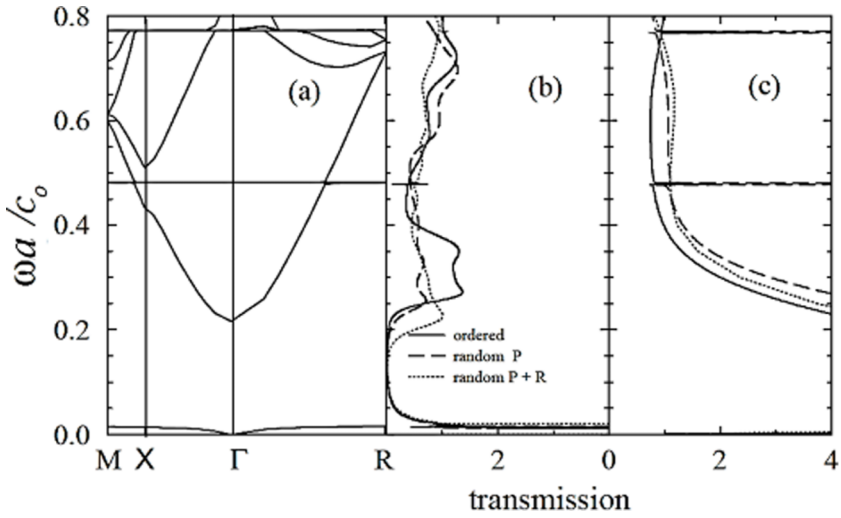

FIG. 8. (a) Band structure of sound propagation in water containing periodically placed bubbles of volume fraction 1% in sc arrangement. (b) Transmission coefficient through a slab of water containing 7 × 7 × 3 bubbles (3 along the incidence direction, considering normal incidence). The transmission is normalized with respect to the transmission coefficient of the same slab of water without bubbles. The continuous line is for periodic placement of identical bubbles, the dashed line is for random placement of identical bubbles, and the dotted line is for random placement of bubbles the radius of which varies randomly. (c) The same as in (b) but by neglecting multiple scattering effects (see text). The figure is reprinted with permission from Ref. 11. Copyright (2000) by American Physical Society.

would imply a gap in all directions. Of course, spherical symmetry and Bravais lattice are incompatible. The lattice structures closer to a spherical symmetry are the close-packed ones such as fcc or hcp. Therefore, it is reasonable to expect that the most favorable (for gap creation) structures are the fcc and the hcp. This expectation is realized for the scalar Helmholtz equation and for acoustic and elastic waves. However, it turns out that for EM waves the most favorable (for gap creation) lattice structure is the diamond one (or diamond-like),[21] in spite of the fact that it is an open structure with only four nearest neighbors and as far away from a spherical symmetry as possible. Apparently, this unexpected behavior must be related with the exclusively transverse character of EM waves and the absence of s-wave scattering from spherical objects.[25] However, to the best of our knowledge, no explicit explanation for this "peculiar" behavior of EM waves is available.

Another aspect where the EM waves behave differently from the other classical waves is the topology: In acoustic and elastic waves gap formation is favored by the cermet topology (Ref. 4, p. 449) where isolated scatterers are fully surrounded by the host material. On the other hand EM waves form gaps easier for the network topology where the scatterers form a connected network.[7] Again, to the best of our knowledge, there is no explanation for this difference.

V. PHONONIC METAMATERIALS

A. Phononic metamaterials and negative refraction

The last 15 years have witnessed the development and applications of novel composite materials possessing properties not encountered in natural materials. Most impressive among them are the so-called left-handed or negative index metamaterials exhibiting over a frequency range negative permittivity and permeability. As a result new and unexpected phenomena appear, such as negative refraction, flat lenses, violation of the diffraction limit, invisibility cloaking etc. Following these impressive developments for the propagation of EM waves, similar directions were pursued for controlling the flow of acoustic and elastic waves.[26,27] An example is the achievement and demonstration of negative refraction in phononic crystals (see, e.g., Ref. 28), as shown in Fig. 9.

In 1995 Milton and Cherkaev[29,30] showed that all mechanical materials can in principle be synthesized by combining pentamodes. The latter are artificial solids such that the ratio of bulk modulus

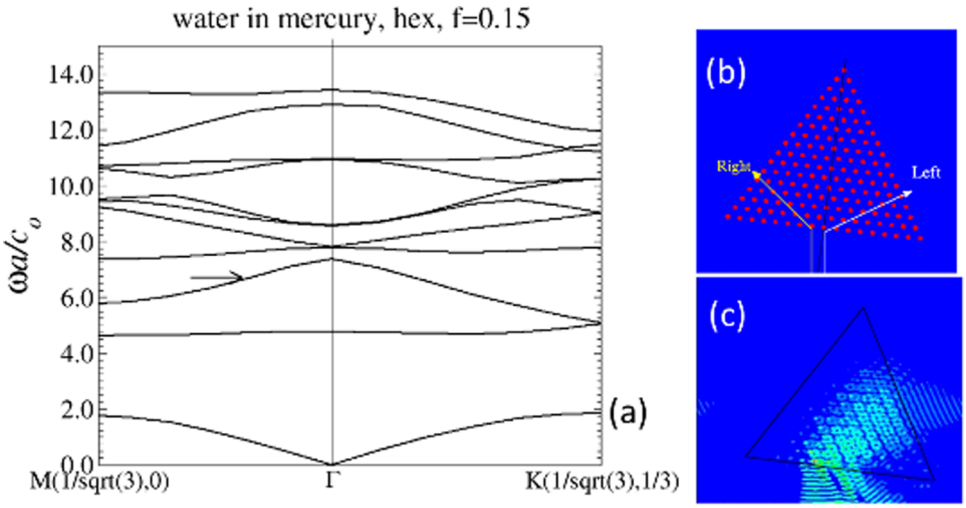

FIG. 9. (a): The band structure of a periodic acoustic system made of water cylinders in mercury in hexagonal; arrangement. Here a is the lattice constant. The cylinder volume fraction is 15%. The band marked by the arrow has negative curvature which indicates opposite phase and group velocity and therefore left-handed behavior and negative refraction (see, e.g., Ref. 28). This negative refraction response is demonstrated in panel (c), where a wave (of dimensionless frequency 7) impinges on a prism-shaped phononic crystal like the one shown in panel (b). In the above calculations the mercury parameters employed are ρ=13500 kgr/m^3, c_l=1531 m/s and the water ones ρ = 1025 kgr/m^3, c_l = 1450 m/s.

to shear modulus is very large, ideally infinite. Pentamodes are the elastic analog of negative index metamaterials in optics. Recently, Kadic *et al.*,[31] by employing the sophisticated technique of dip-in-direct-laser-writing, fabricated a three dimensional structure which approaches the ideal pentamode behavior; the dispersion relations for elastic wave propagation in this structure were calculated[32] and measured,[33] confirming the almost pentamode behavior.

A well-known structure which was studied also as elastic metamaterial[34] is the layer by layer structure shown in Fig. 1. It was found that this structure exhibits a very large ratio of longitudinal to transverse sound velocities, approaching the ideal pentamode behavior. The additional significance

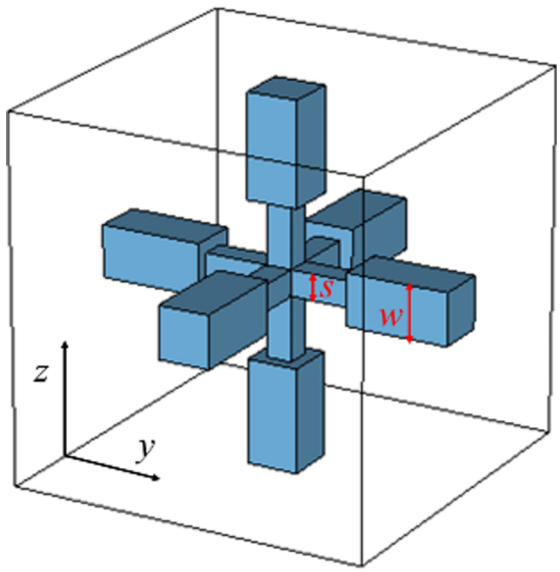

FIG. 10. The computational cell (which is identical to the unit cell) of the new simple cubic structure studied in this work. The width of each rod of square cross-section is symbolized as w at its thick part and s at its thinner part.

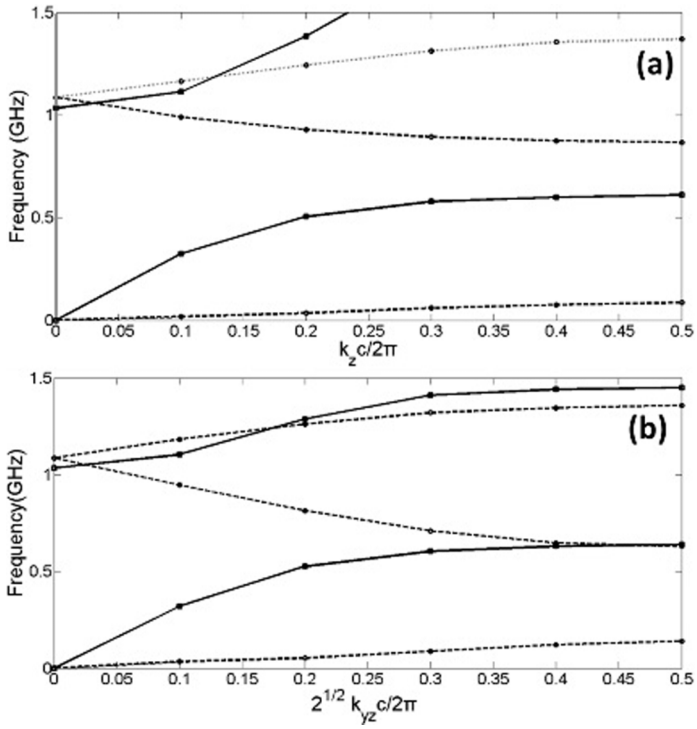

FIG. 11. The band structure of the new simple cubic phononic crystal (see Fig. 10 and the text) for propagation along two different directions. The horizontal axis is the normalized k-vectors along each direction. (a) z-direction (which is the same as the x and y directions due to symmetry) and (b) diagonal direction between y and z axes. Solid line is for the field component along the z-axis, dashed line is for the field component along the x-axis (the component along y-axis is due to symmetry the same as the component along x-axis for case (a) and z-axis for case (b)).

of this result is that the layer-by-layer (a) permits very easy fabrication, and (b) acts as an efficient photonic crystal as well, allowing the possibility of simultaneously molding the flow of both elastic and EM waves.

We report here results for a new structure which was studied as a candidate for pentamode behavior and other interesting elastic metamaterial properties. The structure has a simple cubic symmetry with connecting silicon rods, as shown in Fig. 10. A great advantage of the structure is that it can be also easily fabricated, as the one studied in Ref. 34.

For the *calculation of the band structure* the FDTD method was used. In the calculations only one unit cell was employed with Periodic Boundary Conditions (PBC) along each direction, as a result of the Bloch theorem. The excitation, taken as a Gaussian pulse in time, was located at one low symmetry point of the unit cell. The components of the displacement vector as a function of time were collected in the detection point (in another low symmetry point of the unit cell). However, the results are not dependent on the location of the excitation or the detection point. Each component was Fourier transformed. The resulted spectrum consisted of well-defined resonant peaks that correspond to band structure points for the particular **k** vector. The dimensionless **k** vector components along the three examined directions in k space are defined as $k_y = 2\pi/c$, $k_z = 2\pi/c$ and $k_{yz} = 2\pi/\sqrt{2}c$ respectively, where c is the unit cell size along the three unit cell directions. Changing the **k** vector value used in the PBC, the band structure could be obtained. In our calculations the highest value of the **k** vector was 0.5 starting from 0 and the step size was 0.1. Due to the cubic grid used in the FDTD calculations, a 3D orthogonal lattice was used as computational cell (coinciding with the irreducible cell) consisting of 120 by 120 by 120 grid points along x, y, and z axes, respectively.

The phase velocities of the longitudinal and transverse waves propagating in the structure could be calculated from the slopes of the branches emerging from the Γ (k=0) point of the band structure. This is an accurate calculation in the limit of very small values of k vector. The calculation of the phase

TABLE I. Results of the silicon simple cubic structure of Fig. 10 with c=1μm and w/c=20/120, for different s/c ratios. For each field component the index l-l or t-l indicates the longitudinal-like and transverse-like modes of the field respectively.

s/c	Direction	field component	slope	c_l/c_t
8/120	k_z	x (t-l)	0.175	14.5
8/120	k_z	y (t-l)	0.175	14.5
8/120	k_z	z (l-l)	2.541	
8/120	k_{yz}	x (t-l)	0.263	9.99
8/120	k_{yz}	y (l-l)	2.628	1.00
8/120	k_{yz}	z (l-l)	2.628	
10/120	k_z	x (t-l)	0.306	9.87
10/120	k_z	y (t-l)	0.306	9.87
10/120	k_z	z (l-l)	3.022	
10/120	k_{yz}	x (t-l)	0.438	7.20
10/120	k_{yz}	y (l-l)	3.154	1.00
10/120	k_{yz}	z (l-l)	3.154	
12/120	k_z	x (t-l)	0.394	8.78
12/120	k_z	y (t-l)	0.394	8.78
12/120	k_z	z (l-l)	3.460	
12/120	k_{yz}	x (t-l)	0.569	6.31
12/120	k_{yz}	y (l-l)	3.592	1.00
12/120	k_{yz}	z (l-l)	3.592	
14/120	k_z	x (t-l)	0.482	7.91
14/120	k_z	y (t-l)	0.482	7.91
14/120	k_z	z (l-l)	3.811	
14/120	k_{yz}	x (t-l)	0.701	5.69
14/120	k_{yz}	y (l-l)	3.986	1.00
14/120	k_{yz}	z (l-l)	3.986	

velocities from the band structures could give information about the parameters of the structure that affect each velocity. Silicon is the material considered for this structure which is assumed an isotropic material for the calculations of this work. Notice that an incident longitudinal wave will develop in general transverse components as well, as it propagates through the structure; so it is more accurate to speak for "longitudinal-like" and "transverse-like" components of the field.

A characteristic band structure result of the new structure is shown in Fig. 11. The band-structure was calculated for c=1μm, w/c=20/120 and s/c=8/120, where w is the width of each rod at its thicker part and s the width of each rod at its thinner edge. In all cases the length of the thinner section of the rods is $c/3$ (see Fig. 10). It should be mentioned here that the results can be scaled inversely proportional to the lengths. As can be clearly seen from Fig. 11 the slope of the transverse-like modes (dashed lines) is significantly smaller than the slope of the longitudinal-like modes (solid lines) when frequency tends to zero. There is also a wide frequency region, from about 0.2 to 0.6 GHz, where only the longitudinal-like mode exists in both directions. It is important to mention here that x, y and z directions are by symmetry equivalent; for that reason only results for the k_z and k_{yz} direction are shown. k_{yz} indicates the diagonal direction between y and z axes.

Performing additional calculations for several values of s/c (keeping c=1μm, w/c=20/120 and length of the thinner section of the rods $c/3$) and examining how the velocity of each component of the wave is affected by changing the ratio s/c, we found the results presented in Table I. (It should be mentioned here that the results can be scaled in any other value of c, assuming that the sound velocities and density are independent of frequency.) We considered values for s/c equal 8/120, 10/120, 12/120, 14/120. The ratio of the longitudinal wave velocity over the transverse velocity in each case is shown in the last column of the Table I. We can clearly see that for s/c=8/120 and the k_z direction the ratio c_l/c_t reaches the value 14.5, which is higher than the values achieved by employing the structure of Ref. 34.

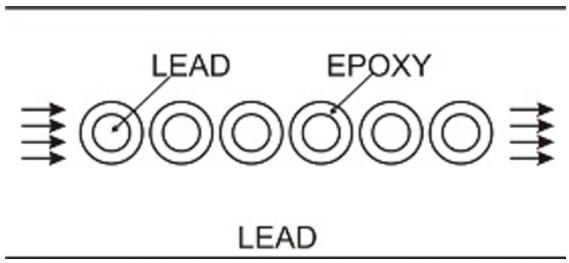

FIG. 12. A structure exhibiting confined propagation by linear combination of resonances. The radii of the internal and the external spheres are 80 mm and 100 mm respectively. The nearest neighbor distance is d=250 mm.

The high c_l/c_t values achievable with the new structure along with its ease in fabrication make it a promising pentamode-like elastodynamic metamaterial.

B. Propagation through linear combination of resonances

In a recent publication[35] the propagation of EM waves along a series of inclusions embedded in a host of permittivity (ε) near zero (ENZ) was studied. It was shown that this propagation takes place by hopping from one inclusion to the next through utilization of resonances in a way analogous to the linear combination of atomic orbitals (LCAO) in electronic wavefunctions in solids. The role of atomic orbitals is played by the resonances; the electric field at those resonances is well localized around the inclusions, resembling the form of p-like atomic orbitals directed along the propagation direction. In the present work we demonstrate a way of propagation of elastic waves which is quite similar to that of Ref. 35. The system consists of a series of lead spheres coated by epoxy and arranged periodically in a straight line within a lead host, as shown in Fig. 12.

In Fig. 13(a) the scattering cross-section by a single coated sphere embedded in lead is shown. A strong resonance can be seen for transverse incidence wave, appearing at f=3.14 kHz.

The absolute value of the displacement field at that resonance is shown in Fig. 13(b). Notice that the field is strongly confined within the coated sphere, in particular around the internal interface. In the perpendicular to the incidence direction there is almost zero escape of the field. On the other hand, the incidence direction is the only one where the field extends outside the coated sphere to some non-negligible degree, by developing the two lobes reminiscent of the p-type atomic orbitals. As a result of this behavior we expect a strongly confined propagation along the chain, similar to the one observed in aromatic hydrocarbons (e.g. benzene), or in graphene ribbons, or in the system studied in Ref. 35. Indeed this is the case as shown in Fig. 14, where the propagation of an elastic wave along

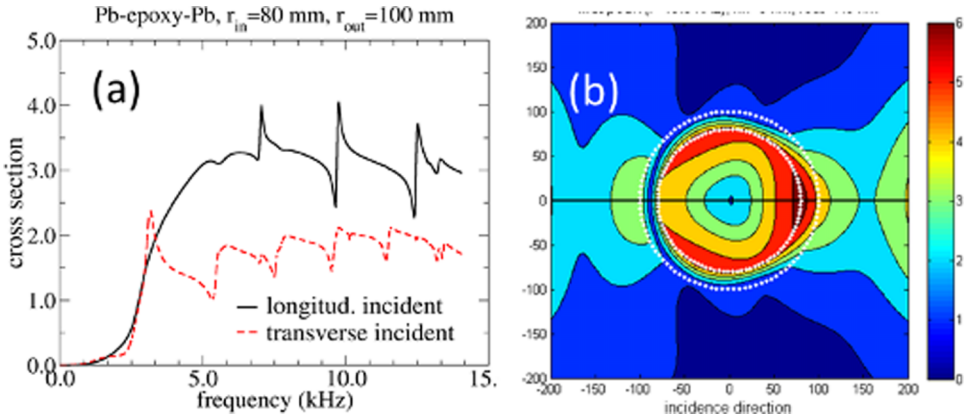

FIG. 13. (a): The scattering cross-section by a single coated sphere of Fig. 12 for longitudinal and transverse incident elastic waves. Notice the strong resonance for transverse incidence, at f=3.14 kHz. (b): The absolute value of the displacement field at the 3.14 kHz resonance shown in panel (a).

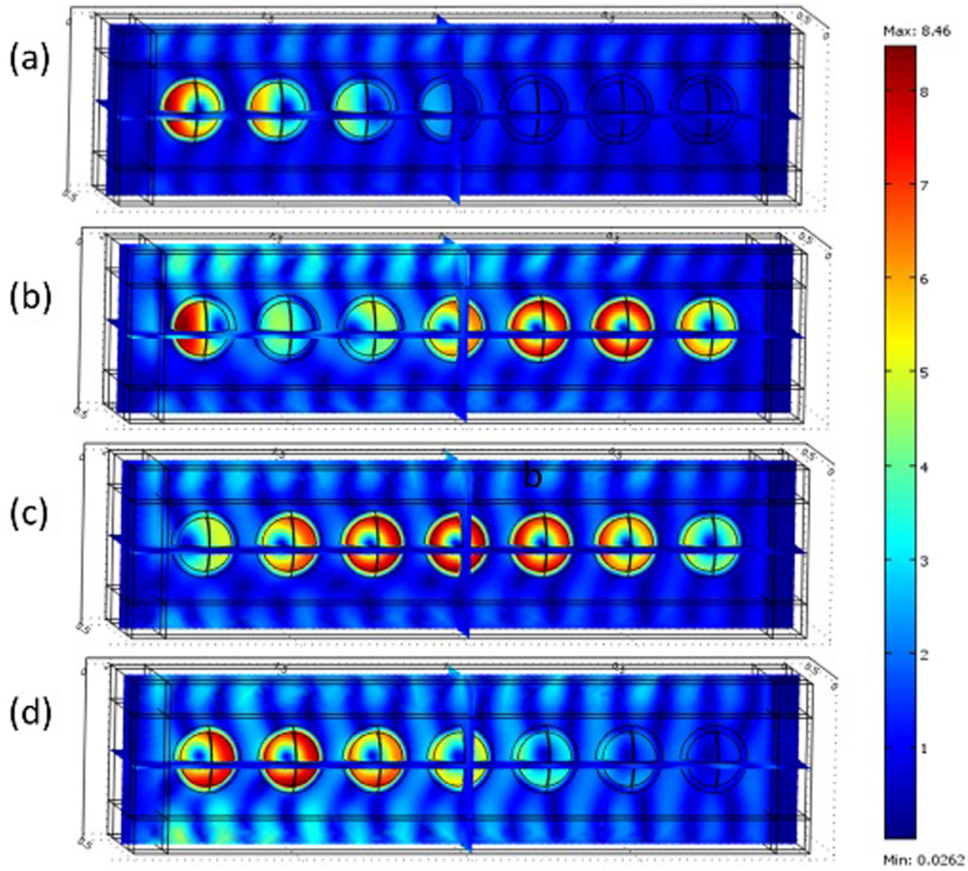

FIG. 14. Propagation of elastic waves along a chain of seven coated spheres as in Fig. 12 for four different frequencies around the f=3.14 kHz resonance discussed in Fig. 13(a): f=3.08 kHz (a), f=3.11 kHz (b), f=3.14 kHz (c) and f=3.17 kHz (d). The result has been obtained using the Finite Element Method (via COMSOL Multiphysics commercial software).

a chain of seven coated spheres, as shown in Fig. 12, is demonstrated, for various frequencies around the f=3.14 kHz resonance.

C. Liquid sensors based on the layer-by-layer structure

In this part of our work the well-known layer-by-layer structure (see Fig. 1) is studied for the first time as a candidate for liquid sensor. This study is prompted by recent results[36,37] showing that phononic crystals are offering an innovating platform for acoustic liquid sensors.

To examine and demonstrate the sensor capabilities of the structure we examine the transmission properties of the structure if it is immersed in different liquids. For this study, where we used the 3D FDTD method, we employed a sample of four unit cells in the stacking direction (z-direction in Fig. 1). Each unit cell contains 4 rods of thickness w_s along the stacking direction. The rod-material is considered as silicon, while the same material is placed on top and bottom of the structure in the stacking direction (the structure is considered as infinite in the x-y plane - see Fig. 1).

Fig. 15 shows the transmission properties of the structure if it is immersed in air, water, propanol and a hypothetical liquid (Liquid 1) for x polarized incident pulse. The material parameters of those materials are listed in Table II. The calculations are for rod distance d =1mm (c/d =40/30, w/d =10/30 and w_s/d =10/30) but the results can be scaled to any other value of d assuming that the sound velocities and density are independent of frequency.

The results for the air case (black line in Fig. 15) show a first gap at between 1.23 MHz and 2.82 MHz, and a second one between 3.2 and ~6 MHz. It is clear from the transmission spectrum

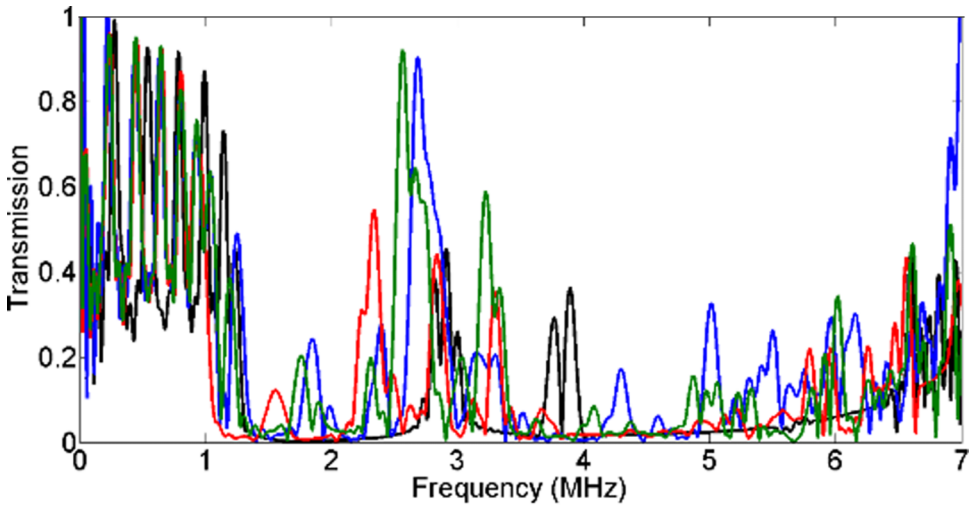

FIG. 15. The transmission as a function of frequency for the layer by layer structure (see Fig. 1) immersed into air (black line) and different liquids for x-polarized incident pulse (which is identical for y polarized pulse due to the symmetry of the structure). For each figure w/d=10/30; the liquids which were tested are water, propanol and liquid 1 (blue, red and green lines respectively).

TABLE II. The longitudinal (c_l), transverse (c_t) sound velocities and the densities for the materials used in the liquid sensor study shown in Fig. 15.

Material	c_l (m/s)	c_t (m/s)	Density (kg/m^3)
Liquid 1	1421	-	908
Propanol	1220	-	804
Silicon	8430	5840	2340
Water	1497	-	1000
Air	331	-	1.29

that there is a significant change on the band gaps edges when different liquids are considered. We can also observe that for x-polarized pulse, transmission peaks appear inside the air band gaps when liquid replaces air, and the position of these peaks depends strongly on the liquid considered. E.g., focusing on the first gap, for water there is a peak at frequency 1.846 MHz, which for propanol moves to 1.758 MHz and for Liquid 1 to 1.553 MHz. The obvious dependence of the frequency of each transmission peak within each band gap on the liquid considered shows that the structure is a promising candidate for liquid sensor applications.

Another parameter that can be used for sensing applications can be the significant change of the upper edge of the first band gap when different liquids are considered. This band edge is at frequencies 2.82MHz for the air case, 2.68MHz for water, 2.56MHz for liquid 1 and 2.33MHz for propanol. So it is obvious that when the structure is immersed into different liquids the change of upper edge of the first bang gap could give information for the liquid that the structure is immersed to.

VI. CONCLUSIONS

In the present paper the early work on phononic crystals is discussed and the content of initial paper on this subject is briefly presented. The central role of resonances (either geometric or of inherent material nature) for the creation of gaps is reviewed. The various equations governing wave propagation of (a) electrons in solids (Schrödinger equation), (b) acoustic waves in fluids, (c) elastic waves in solids treated as continuous media, and (d) electromagnetic (EM) waves in matter and in vacuum, are written down in order to exploit possible mathematical equivalences and to point out their differences. As an example of the consequences of equivalences we mention the conclusion that a local region of

low sound velocity in fluids is the analog of a potential well for electrons moving within a solid. As far as the differences are concerned it is worth to mention that gap formation for EM waves is favored by the network topology and by open lattice structures such as the diamond and diamond-like ones. In contrast, for acoustic and elastic waves gap formation is favored by cermet topology (where each inclusion is fully surrounded by the host material) and by close-packed lattices such as fcc, or hcp. It is thought that these impressive differences are connected with the absence of longitudinal component in the EM waves, although no convincing explanation seems to exist. Material conditions favoring wide gaps for elastic waves are heavy inclusions in light host, such as, e.g., tungsten in epoxy. One can explain such a behavior by comparing the scattering cross-section by a single inclusion with the one by a rigid inclusion; this analysis reveals that there two channels of propagation, one employing the host material almost exclusively and the other by hopping from inclusion to inclusion employing the resonances in analogy with electron propagation in solids employing the atomic orbitals. This analysis was attempted in the opposite case of a light inclusion in a heavy host. By comparing with the results of a recent experiment, it was found that the above presented picture is not applicable to the case of light-inclusions/heavy-host situation apparently because a third mixed channel of propagation exists with the field concentrated near the interfaces. An interesting extreme case of the light-inclusion/heavy-host case is that of bubbly water where the very strong so-called Minnaert resonance dominates the sound propagation and induces a large gap due to multiple scattering events.

In the last part of the paper several cases of phononic metamaterials were studied. Some of them exhibit negative refraction. Others, such as the well-known in the field of photonic crystals layer-by layer structure, show pentamode-type behavior; this behavior is important for realizing transformation elastodynamics and possibly elastic wave cloaking. The same structure was studied as liquid sensor. Finally, an elastic system was designed and studied behaving in a way analogous to the EM case where the host has permittivity ε almost zero (ENZ) and the EM wave propagates along a narrow channel following a linear chain of inclusions by hopping from inclusion to inclusion by employing strongly localized resonances of p-type symmetry.

ACKNOWLEDGEMENTS

The work is partially supported by the ERC grant PHOTOMETA and by "Karatheodoris" Research Program of the University of Patras. The research has been also co-financed by the EU (European Regional Development Fund – ERDF) and Greek national funds through Operational Program "Regional Operational Programme" of the National Strategic Reference Framework (NSRF) – Research Funding Program: Support for research, technology and innovation actions in Region of Western Greece. Authors acknowledge C. M. Soukoulis at Iowa State University for useful discussions and the realization of COMSOL simulations.

[1] I. Newton, *Principia*, Book II, 1686.
[2] L. Brillouin, *Wave Propagation in Periodic Structures*, 2nd ed. (Dover Publ., N.Y., 1953).
[3] Proceedings of the Royal Society of London, series A, Vol. **371**, pp. 1-177, *The Beginnings of Solid State Physics*.
[4] E. N. Economou, *The Physics of Solids: Essentials and Beyond* (Springer, Berlin, 2010).
[5] P.W. Anderson, "Absence of Diffusion in Certain Random Lattices," Phys. Rev. **109**, 1492 (1958).
[6] E. Yablonovitch and T. J. Gmitter, "Photonic band structure: The face-centered-cubic case," Phys. Rev. Lett. **63**, 1950 (1989).
[7] K. M. Ho, C. T. Chan, and C. M. Soukoulis, "Existence of a photonic gap in periodic dielectric structures," Phys. Rev. Lett. **65**, 3152 (1990).
[8] K. M. Ho, C. T. Chan, C. M. Soukoulis, R. Biswas, and M. Sigalas, "Photonic band gaps in three dimensions: New layer-by-layer periodic structures," Sol. State Commun. **89**, 413 (1994).
[9] J. D. Joannopoulos *et al.*, *Photonic Crystals: Molding the Flow of Light*, 2nd ed. (Princeton University Press, Princeton, 2008).
[10] M. M. Sigalas and E. N. Economou, "Elastic and acoustic wave band structure," J. of Sound and Vibrations **158**, 377-382 (1992).
[11] M. Kafesaki, R. S. Penciu, and E. N. Economou, "Air bubbles in water: a strongly multiple scattering medium for acoustic waves," Phys. Rev. Lett. **84**, 6050 (2000).
[12] E. Özbay, A. Abeyta, G. Tuttle, M. Tringides, R. Biswas, C. T. Chan, C. M. Soukoulis, and K. M. Ho, "Measurement of a three-dimensional photonic band gap in a crystal structure made of dielectric rods," Phys. Rev. B **50**, 1945 (1994).
[13] M. Kafesaki and E. N. Economou, "Interpretation of the band structure results for elastic and acoustic waves by analogy with the LCAO approach," Phys. Rev. B **52**, 13317-13331 (1995).
[14] Z. Liu, X. Zhang, Y. Mao, Y. Y. Zhu, Z. Yang, C. T. Chan, and P. Sheng, "Locally resonant sonic materials," Science **289**, 1734 (2000).

[15] Landau and Lifshitz, *Theory of Elasticity*, 3rd ed. (Pergamon Press, Oxford, 1986).
[16] M. Kafesaki and E. N. Economou, "Multiple scattering theory for 3D periodic acoustic composites," Phys. Rev. B **60**, 11993 (1999).
[17] J. H. Page, Ping Sheng, H. P. Schriemer, I. Jones, Xiaodun Jing, and D. A. Weitz, "Group Velocity in Strongly Scattering Media," Science **271**, 634 (1990).
[18] R. Sainidou, N. Stefanou, E. Psarobas, and A. Modinos, "A layer-multiple-scattering method for phononic crystals and heterostructures of such," Comp. Phys. Comm. **166**, 197 (2005).
[19] E. N. Economou, *Green's functions in Quantum Physics*, 3rd ed. (Springer Verlag, 2006).
[20] E. N. Economou and A. Zdetsis, "Classical wave propagation in periodic structures," Phys. Rev. B **40**, 1334 (1989).
[21] E. N. Economou and M. M. Sigalas, "Stop bands for elastic waves in periodic composite materials," J. Acoust. Soc. Am. **95**, 1735 (1994).
[22] M. Sigalas, M. S. Kushwaha, E. N. Economou, M. Kafesaki, I. E. Psarobas, and W. Steurer, "Classical vibrational modes in photonic lattices: theory and experiment," Zeitschrift fur Kristallographie **220**, 765-809 (2005).
[23] M. Kafesaki, E. N. Economou, and M. M. Sigalas, in *Photonic Band gap Materials*, edited by C.M. Soukoulis (Kluwer, Dordrecht, 1996), pp. 143-164.
[24] A. Sato, Y. Pennec, T. Yanagishita, H. Masuda, W. Knoll, B. Djafari-Rouhani, and G. Fytas, "Cavity-type hypersonic phononic crystals," New Journal of Physics **14**, 113032 (2012), Fig. 5(a).
[25] J. A. Stratton, *Electromagnetic Theory* (McGraw-Hill, New York, 1941), pp. 563-573.
[26] *Acoustic Metamaterials and Phononic Crystals*, edited by P.A. Deymier (Springer, Berlin, 2013).
[27] M.I. Hussein, M. J. Leamy, and M. Ruzzene, "Closure to Discussion of 'Dynamics of Phononic Materials and Structures: Historical Origins, Recent Progress, and Future Outlook," Appl. Mech. Rev. **66**, 040802 (2014).
[28] X. Zhang and Z. Liu, "Negative refraction of acoustic waves in two-dimensional phononic crystals," Appl. Phys. Lett. **85**, 341 (2004).
[29] G.W. Milton and A. Cherkaev, "Which elasticity tensors are realizable," J. of Eng. Mater. Techn **117**, 483 (1995).
[30] G. W. Milton, *The Theory of Composites* (Cambridge University Press, Cambridge, 2002).
[31] M. Kadic, T. Buckmann, N. Stenger, M. Thiel, and M. Wegener, "On the practicability of pentamode mechanical metamaterials," Appl. Phys. Lett. **100**, 191901 (2012).
[32] A. Martin, M. Kadic, R. Schittny, T. Buckmann, and M. Wegener, "Phonon band structure of three-dimensional pentamode metamaterials," Phys. Rev. B **86**, 155116 (2012).
[33] R. Schittny *et al.*, "Three-dimensional labyrinthine acoustic metamaterials," Appl. Phys. Lett. **103**, 231905 (2013).
[34] N. Aravantinos-Zafiris, M. M. Sigalas, and E. N. Economou, "Elastodynamic behavior of the three dimensional layer-by-layer metamaterial structure," Journal of Applied Physics (to appear).
[35] A. A. Basharin, Ch. Mavidis, M. Kafesaki, E. N. Economou, and C. M. Soukoulis, "Epsilon near zero based phenomena in metamaterials," Phys. Rev. B **87**, 155130 (2013).
[36] R. Lucklum and J. Li, "Phononic crystals for liquid sensor applications," Measurement Science and Technology **20**, 124014 (2009).
[37] R. Lucklum, M. Kea, and M. Zubtsova, "Two-dimensional phononic crystal sensor based on a cavity mode," Sensors and Actuators B **171-172**, 271 (2012).